PNAS
www.pnas.org

Supplementary Information for

Blood-based untargeted metabolomics in Relapsing-Remitting Multiple Sclerosis revealed the testable therapeutic target

Insha Zahoor,[1*] Hamid Suhail,[1*] Indrani Datta,[2] Mohammad Ejaz Ahmed,[1] Laila M Poisson,[2] Jeffrey Waters,[1] Faraz Rashid,[1] Rui Bin,[1] Jaspreet Singh,[1] Mirela Cerghet,[1] Ashok Kumar,[3] Md Nasrul Hoda,[1] Ramandeep Rattan,[4] Ashutosh K Mangalam,[5] and Shailendra Giri[1*]

Paste corresponding author: Shailendra Giri
Email: sgiri1@hfhs.org

Top Canonical Pathways		
Name	p-value	Overlap
Sphingosine and Sphingosine-1-phosphate Metabolism	4.35E-03	20.0 % 2/10
TCA Cycle II (Eukaryotic)	1.41E-02	11.1 % 2/18
Renal Cell Carcinoma Signaling	2.08E-02	50.0 % 1/2
Ceramide Signaling	4.12E-02	25.0 % 1/4
Sphingosine-1-phosphate Signaling	4.12E-02	25.0 % 1/4

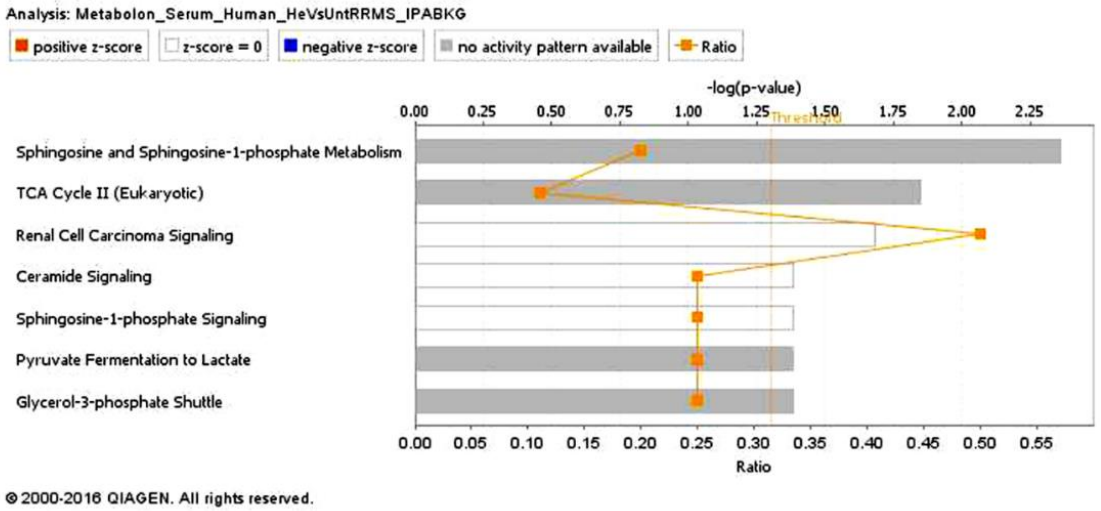

Fig. S1. Top canonical pathways identified in metabolomics of RRMS patients using Ingenuity Pathway Analysis.

Top Networks		
ID	Associated Network Functions	Score
1	Cell Signaling, Molecular Transport, Vitamin and Mineral Metabolism	33
2	Lipid Metabolism, Molecular Transport, Small Molecule Biochemistry	13
3	Hereditary Disorder, Lipid Metabolism, Molecular Transport	3

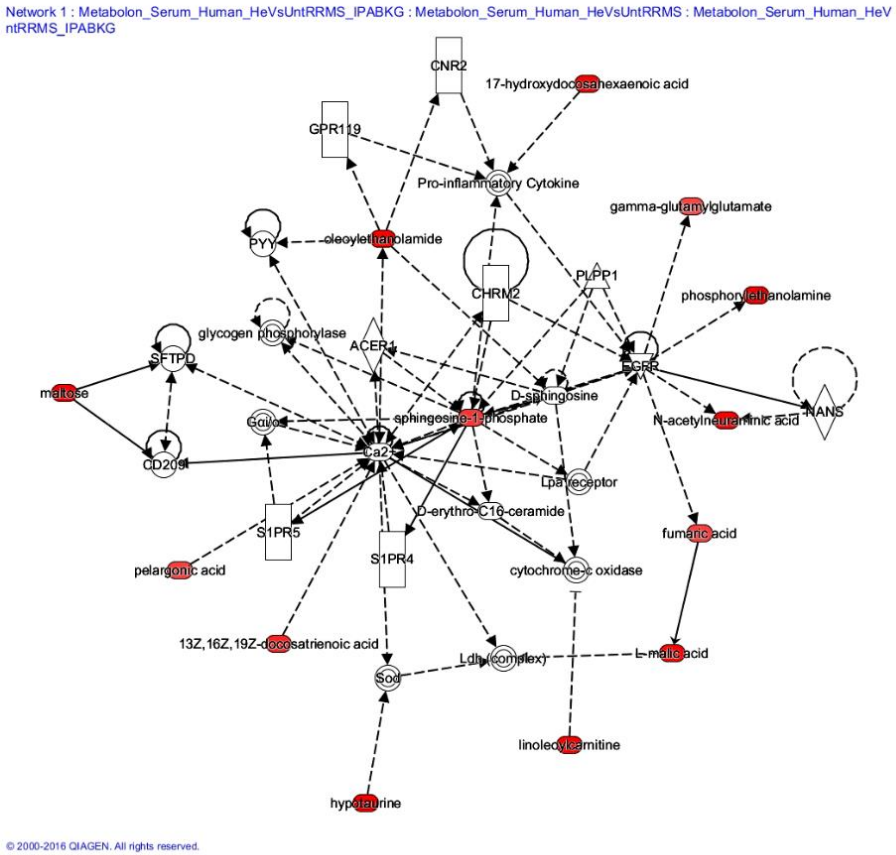

Fig. S2. Cell signaling, molecular transport, vitamin and mineral metabolism (score 33 with 13 focus molecules), top networks identified by IPA.

Table S1: Demographic information of healthy and RRMS patients

	Healthy **(N=14)**	**RRMS** **(N=35)**
Female, N (%)	64%	64%
Mean age, years	40	45
Mean disease duration	--	18.2 yrs
DMTs treatment	NA	None

DMT, Disease modifying therapies; NA, Not applicable; RRMS, Relapsing-remitting multiple sclerosis.

Table S2. Significantly altered metabolites in serum of RRMS vs. healthy.

BIOCHEMICAL	SUPER.PATHWAY	SUB.PATHWAY	KEGG	Group.HMDB	T.Stat	Pval.T	Pval.W	Qval.T	Qval.W
hypotaurine	Amino Acid	Methionine, Cysteine, SAM and Taurine Metabolism	C00519	HMDB00965	4.4309	0.0001	0.0007	0.0228	0.1469
phosphoethanolamine	Lipid	Phospholipid Metabolism	C00346	HMDB00224	4.2791	0.0001	0.0016	0.0228	0.1469
ADSGEGDFXAEGGGVR*	Peptide	Fibrinogen Cleavage Peptide			4.0188	0.0002	0.0027	0.0289	0.1729
gamma-tocopherol	Cofactors and Vitamins	Tocopherol Metabolism	C02483	HMDB01492	3.7585	0.0006	0.0018	0.0611	0.1469
oleic ethanolamide	Lipid	Endocannabinoid		HMDB02088	3.6414	0.0009	0.0018	0.0699	0.1469
DSGEGDFXAEGGGVR*	Peptide	Fibrinogen Cleavage Peptide			3.5060	0.0012	0.0047	0.0699	0.2105
glycerophosphoethanolamine	Lipid	Phospholipid Metabolism	C01233	HMDB00114	3.4792	0.0012	0.0095	0.0699	0.2670
N-acetylmethionine	Amino Acid	Methionine, Cysteine, SAM and Taurine Metabolism	C02712	HMDB11745	3.3886	0.0015	0.0321	0.0736	0.4772
maltose	Carbohydrate	Glycogen Metabolism	C00208	HMDB00163	3.2586	0.0026	0.0222	0.1030	0.3824
N-acetylneuraminate	Carbohydrate	Aminosugar Metabolism	C00270	HMDB00230	3.2410	0.0023	0.0527	0.1013	0.5132
allo-isoleucine	Amino Acid	Leucine, Isoleucine and Valine Metabolism		HMDB00557	3.1433	0.0034	0.0102	0.1204	0.2673
linoleoylcarnitine*	Lipid	Fatty Acid Metabolism(Acyl Carnitine)		HMDB06469	2.9921	0.0045	0.0606	0.1477	0.5403
17-HDoHe	Lipid	Fatty Acid, Monohydroxy		HMDB10213	2.9670	0.0056	0.0097	0.1690	0.2670
glutamine-leucine	Peptide	Dipeptide		HMDB28801	2.8187	0.0071	0.0081	0.2014	0.2670
malate	Energy	TCA Cycle	C00149	HMDB00156	2.7913	0.0078	0.0432	0.2053	0.5132
leucylglutamine*	Peptide	Dipeptide		HMDB28927	2.7078	0.0096	0.0185	0.2357	0.3401
lactate	Carbohydrate	Glycolysis, Gluconeogenesis, and Pyruvate Metabolism	C00186	HMDB00190	2.6968	0.0103	0.0112	0.2399	0.2825

2-methoxyacetaminophen sulfate*	Xenobiotics	Drug		HMDB62550	2.6782	0.0116	0.0165	0.2407	0.3382
pregnanediol-3-glucuronide	Lipid	Steroid		HMDB10318	2.6622	0.0115	0.0188	0.2407	0.3401
3-(cystein-S-yl)acetaminophen*	Xenobiotics	Drug		HMDB240217	2.6435	0.0126	0.0740	0.2486	0.5564
valylglycine	Peptide	Dipeptide		HMDB29127	2.5775	0.0133	0.0343	0.2503	0.4966
gabapentin	Xenobiotics	Drug	D00332	HMDB05015	2.5583	0.0155	0.0486	0.2773	0.5132
palmitoleoyl sphingomyelin (16:1)*	Lipid	Sphingolipid Metabolism			2.5431	0.0180	0.0169	0.2831	0.3382
chiro-inositol	Lipid	Inositol Metabolism	C19891	HMDB34220	2.5213	0.0164	0.3188	0.2816	0.8187
threonylphenylalanine	Peptide	Dipeptide		HMDB29068	2.4826	0.0178	0.0132	0.2831	0.3060
2-methoxyacetaminophen glucuronide*	Xenobiotics	Drug		HMDB240215	2.4566	0.0196	0.0740	0.2831	0.5564
docosatrienoate (22:3n3)	Lipid	Polyunsaturated Fatty Acid (n3 and n6)	C16534	HMDB02823	2.4111	0.0201	0.0644	0.2831	0.5403
3-(N-acetyl-L-cystein-S-yl) acetaminophen	Xenobiotics	Drug			2.4084	0.0220	0.0740	0.2831	0.5564
glycerol 3-phosphate (G3P)	Lipid	Glycerolipid Metabolism	C00093	HMDB00126	2.3895	0.0212	0.1492	0.2831	0.7261
1-oleoylplasmenylethanolamine*	Lipid	Lysolipid			2.3687	0.0222	0.3385	0.2831	0.8187
L-urobilin	Cofactors and Vitamins	Hemoglobin and Porphyrin Metabolism	C05793	HMDB04159	2.3417	0.0253	0.0441	0.2915	0.5132
orotidine	Nucleotide	Pyrimidine Metabolism, Orotate containing	C01103	HMDB00788	2.3416	0.0250	0.0298	0.2915	0.4538
5alpha-pregnan-3beta,20alpha-diol monosulfate (2)	Lipid	Steroid			2.3212	0.0261	0.4971	0.2915	0.8367
stearoylcarnitine	Lipid	Fatty Acid Metabolism(Acyl Carnitine)		HMDB00848	2.2770	0.0291	0.0413	0.2915	0.5132

3-hydroxybutyrate (BHBA)	Lipid	Ketone Bodies	C01089	HMDB00357	2.2600	0.0295	0.4003	0.2915	0.8198
4-androsten-3beta,17beta-diol monosulfate (2)	Lipid	Steroid			2.2514	0.0293	0.1428	0.2915	0.7189
docosadienoate (22:2n6)	Lipid	Polyunsaturated Fatty Acid (n3 and n6)	C16533	HMDB61714	2.2505	0.0295	0.4267	0.2915	0.8198
betonicine	Xenobiotics	Food Component/Plant	C08269	HMDB29412	2.2206	0.0325	0.2889	0.3073	0.8187
sphingosine 1-phosphate	Lipid	Sphingolipid Metabolism	C06124	HMDB00277	2.2181	0.0365	0.0009	0.3073	0.1469
5alpha-pregnan-3beta,20alpha-diol disulfate	Lipid	Steroid			2.2112	0.0327	0.2727	0.3073	0.8187
5alpha-pregnan-3(alpha or beta),20beta-diol disulfate	Lipid	Steroid			2.1812	0.0350	0.6457	0.3073	0.8950
adipate	Lipid	Fatty Acid, Dicarboxylate	C06104	HMDB00448	2.1745	0.0369	0.0148	0.3073	0.3292
oleoylcarnitine	Lipid	Fatty Acid Metabolism(Acyl Carnitine)		HMDB05065	2.1655	0.0361	0.2340	0.3073	0.8187
pregnanolone/allopregnanolone sulfate	Lipid	Steroid			2.1524	0.0382	0.2418	0.3073	0.8187
fumarate	Energy	TCA Cycle	C00122	HMDB00134	2.1428	0.0379	0.1756	0.3073	0.7547
pelargonate (9:0)	Lipid	Medium Chain Fatty Acid	C01601	HMDB00847	2.1217	0.0395	0.5730	0.3097	0.8668
5alpha-androstan-3alpha,17beta-diol monosulfate (1)	Lipid	Steroid			2.0968	0.0417	0.1661	0.3097	0.7437
2-stearoylglycerophosphocholine*	Lipid	Lysolipid			2.0638	0.0449	0.1611	0.3097	0.7437
gamma-glutamylglutamate	Peptide	Gamma-glutamyl Amino Acid	C05282	HMDB11737	2.0609	0.0452	0.1911	0.3097	0.7773
cis-vaccenate (18:1n7)	Lipid	Long Chain Fatty Acid	C08367	HMDB03231	2.0600	0.0458	0.1410	0.3097	0.7162
4-acetamidophenol	Xenobiotics	Drug	C06804	HMDB01859	2.0539	0.0482	0.0402	0.3097	0.5132

2-palmitoylglycerophosphocholine*	Lipid	Lysolipid		HMDB61702	2.0430	0.0470	0.1015	0.3097	0.6184
1-palmitoleoylglycerophosphocholine (16:1)*	Lipid	Lysolipid		HMDB10383	2.0400	0.0477	0.0789	0.3097	0.5581
threonate	Cofactors and Vitamins	Ascorbate and Aldarate Metabolism	C01620	HMDB00943	-2.1731	0.0437	0.0749	0.3097	0.5564
N-acetylalliin	Xenobiotics	Food Component/Plant			-2.1793	0.0480	0.0225	0.3097	0.3824
2-aminophenol sulfate	Xenobiotics	Chemical		HMDB61116	-2.2367	0.0415	0.0056	0.3097	0.2175
iminodiacetate (IDA)	Xenobiotics	Chemical	C19911	HMDB11753	-2.2642	0.0381	0.0053	0.3073	0.2175
tartronate (hydroxymalonate)	Xenobiotics	Bacterial/Fungal	C02287	HMDB35227	-2.3580	0.0270	0.0041	0.2915	0.2105
tiglyl carnitine	Amino Acid	Leucine, Isoleucine and Valine Metabolism		HMDB02366	-2.3903	0.0268	0.0182	0.2915	0.3401
EDTA	Xenobiotics	Chemical	C00284	HMDB15109	-2.4916	0.0210	0.0095	0.2831	0.2670

Master Regulator
S1PR2

Table S3: Casual Network List

TGFB1	Molecule Type	Participating regulators	Depth	Predicted	Notes	Activation z-score	p-value of overlap	Network bias-corrected p-value	Target molecules in dataset	Causal network	Target-connected regulators	Multiple Sclerosis(Length | Paths)	Multiple Sclerosis(Path Types)	relapsed multiple sclerosis [relapse multiple sclerosis](Length | Paths)	relapsed multiple sclerosis [relapse multiple sclerosis](Path Types)	Relationships Between Master Regulators(Increases/Downstream)	Relationships Between Master Regulators(Decreases/Downstream)
nitroaspirin	G-protein coupled receptor	AKT1,Ca2+,CEBPB,ERBB2,IL1B,LIPE,MAPK1,MYC,NFkB (complex),PLC,Rac,S1PR2,Sphk	3	Activated	biased	2.449	9.00E-04	5.20E-03	3-hydroxybutyric acid,fumaric acid,L-lactic acid,oleoylethanolamide,phosphorylethanolamine,sphingosine-1-phosphate	6 (13)	7	3 | 18	DU(13),IU(5)	3 | 1	DU(1)		
dihydrotestosterone	growth factor	ERBB2,FN1,MYC,TGFB1	2	Activated	biased	2.236	1.04E-03	5.50E-03	3-hydroxybutyric acid,fumaric acid,L-lactic acid,phosphorylethanolamine,sphingosine-1-phosphate	5 (4)	4	2 | 1	IU(1)	3 | 38	DU(21),IU(17)	F2,lipopolysaccharide,Pdgf (complex),S1PR2,streptozocin	berberine,CHRNA7,LPA,maslinic acid
ammonia	chemical drug	CASP1,CASP8,ERBB2,IL1B,nitroaspirin,PPARA,PTGS2,STK11,TP53	3	Inhibited	biased	-2.236	1.04E-03	1.90E-03	3-hydroxybutyric acid,fumaric acid,L-lactic acid,phosphorylethanolamine,sphingosine-1-phosphate	5 (9)	5	3 | 2	DU(1),IU(1)	3 | 1	IU(1)		
misoprostol	chemical - endogenous mammalian	dihydrotestosterone,ERBB2,GPD2,TP53	2	Activated		2.000	1.41E-03	2.90E-03	fumaric acid,phosphorylethanolamine,sn-glycerol-3-phosphate,sphingosine-1-phosphate	4 (4)	3	3 | 116	DU(62),IU(54)	3 | 14	DU(5),IU(9)	CSHL1,IGF2,SIAH2	
PTGS2	chemical - endogenous mammalian	ammonia,CEBPB,ERBB2,IL1B,Sphk,SRC (family),TLR4	3	Activated	biased	2.236	1.59E-03	9.40E-03	3-hydroxybutyric acid,fumaric acid,L-lactic acid,phosphorylethanolamine,sphingosine-1-phosphate	5 (7)	4	3 | 3	DU(2),IU(1)	3 | 2	DU(2)		CEBPB
CSNK1A1	chemical drug	Ca2+,ERBB2,ITGAM,LIPE,misoprostol,PLC,PTGER1	3	Activated	biased	2.236	1.84E-03	7.50E-03	3-hydroxybutyric acid,fumaric acid,oleoylethanolamide,phosphorylethanolamine,sphingosine-1-phosphate	5 (7)	4	2 | 1	DU(1)				
WSX1-gp130	enzyme	ERBB2,PPARA,PTGS2,STK11,TP53	2	Activated	biased	2.000	2.14E-03	2.10E-03	3-hydroxybutyric acid,fumaric acid,phosphorylethanolamine,sphingosine-1-phosphate	4 (5)	4	3 | 33	DU(12),IU(21)	3 | 6	DU(3),IU(3)	4-methylnitrosoamino-1-(3-pyridinyl)-1-butanone,CASR,CEBPB,cobalt chloride,F2,FYN,Gsk3,IGF2,IKBKB,IL1,ITGAM,lipopolysaccharide,lysophosphatidic acid,misoprostol,NQO1,Pdgf (complex),Pka,S1PR2,streptozocin,TGFB1,TXNIP	ARN2508,ATP,capsazepine,dihydrotestosterone,maslinic acid,N-Ac-Leu-Leu-norleucinal,nitroaspirin,PD 153035,prostaglandin A1,prostaglandin J2,SGPP1,U73122,valdecoxib
IL12RB2	kinase	CHRM3,CSNK1A1,CTNNB1,ERBB2,IL1B,MYC,NFkB (complex),TP53	3	Activated	biased	2.236	2.33E-03	1.72E-02	3-hydroxybutyric acid,fumaric acid,L-lactic acid,phosphorylethanolamine,sphingosine-1-phosphate	5 (8)	5	3 | 23	DU(9),IU(14)	3 | 3	DU(2),IU(1)		
urotensin II	complex	ERBB2,FYN,IFNG,JAK2,STAT4,WSX1-gp130	3	Activated	biased	2.000	2.76E-03	3.40E-03	3-hydroxybutyric acid,fumaric acid,phosphorylethanolamine,sphingosine-1-phosphate	4 (6)	3	3 | 2	IU(2)				
CASR	transmembrane receptor	ERBB2,FYN,IFNG,IL12 (family),IL12RB2,JAK2,STAT4	3	Activated	biased	2.000	2.76E-03	3.00E-03	3-hydroxybutyric acid,fumaric acid,phosphorylethanolamine,sphingosine-1-phosphate	4 (7)	3	3 | 9	DU(7),IU(2)			lipopolysaccharide	
spermine nitric oxide complex	biologic drug	CXCL8,ERBB2,ITGAM,lipase,LIPE,urotensin II	3	Activated	biased	2.000	3.70E-03	9.70E-03	3-hydroxybutyric acid,fumaric acid,phosphorylethanolamine,sphingosine-1-phosphate	4 (6)	3	3 | 2	DU(1),IU(1)	3 | 1	DU(1)		
XRCC5	G-protein coupled receptor	Ca2+,CASR,ERBB2,FYN,IL1B,Inflammasome (Nalp3, Asc, Casp1),PLC,SRC	3	Activated	biased	2.236	4.21E-03	2.89E-02	fumaric acid,L-lactic acid,oleoylethanolamide,phosphorylethanolamine,sphingosine-1-phosphate	5 (8)	4	3 | 27	DU(14),IU(13)	3 | 4	DU(3),IU(1)	ATP,lipopolysaccharide,phenobarbital	NFKBIB,streptozocin
TOPBP1	chemical toxicant	CEBPB,ERBB2,RB1,spermine nitric oxide complex,TP53	3	Inhibited		-2.000	4.36E-03	2.22E-02	3-hydroxybutyric acid,fumaric acid,phosphorylethanolamine,sphingosine-1-phosphate	4 (5)	3	3 | 7	DU(6),IU(1)	3 | 2	DU(2)		
IKBKB	enzyme	Akt,CEBPB,ERBB2,IL1B,NFkB (complex),PRKDC,STK11,TP53,XRCC5	3	Activated	biased	2.236	4.38E-03	2.92E-02	3-hydroxybutyric acid,fumaric acid,L-lactic acid,phosphorylethanolamine,sphingosine-1-phosphate	5 (9)	5	3 | 3	DU(3)	3 | 1	DU(1)	CXCL12	

SOX9	other	CDK2,CEBPB,ERBB2,TOPBP1,TP53	3	Activated		2.000	4.84E-03	1.86E-02	3-hydroxybutyric acid,fumaric acid,phosphorylethanolamine,sphingosine-1-phosphate	4 (5)	3	3 | 9	DU(6),IU(3)	3 | 1	IU(1)		UBR5
RPL23A	kinase	ATM,Ca2+,ERBB2,ERK,IKBKB,IL1B,NCOA3,NFkB (complex),STK11,TNFAIP3,TP53,TRAF6	3	Activated		2.236	4.91E-03	4.57E-02	fumaric acid,L-lactic acid,oleoylethanolamide,phosphorylethanolamine,sphingosine-1-phosphate	5 (12)	5	2 | 6	DU(3),IU(3)	2 | 1	DU(1)	ERBB2,F2,IGF2,IL1,lipopolysaccharide,oltipraz,Pdgf (complex),Rsk	15-deoxy-delta-12,14 -PGJ2,Pka,prostaglandin A1,U73122,UCP2
MELK	transcription regulator	AR,CEBPB,CTNNB1,ERBB2,SOX9,TP53	3	Inhibited		-2.000	5.09E-03	1.37E-02	3-hydroxybutyric acid,fumaric acid,phosphorylethanolamine,sphingosine-1-phosphate	4 (6)	3	3 | 13	DU(10),IU(3)	3 | 3	DU(3)	FN1,IL1,Pka,TGFB1	SMAD6
ATG7	other	CEBPB,ERBB2,RB1,RPL23A,TP53	3	Activated		2.000	5.09E-03	2.09E-02	3-hydroxybutyric acid,fumaric acid,phosphorylethanolamine,sphingosine-1-phosphate	4 (5)	3	3 | 8	DU(4),IU(4)				
TRIM28	kinase	CEBPB,ERBB2,MELK,RB1,TP53	3	Inhibited		-2.000	5.36E-03	2.32E-02	3-hydroxybutyric acid,fumaric acid,phosphorylethanolamine,sphingosine-1-phosphate	4 (5)	3	3 | 2	DU(1),IU(1)	3 | 1	IU(1)		
nandrolone decanoat	enzyme	ATG7,ERBB2,FYN,JAK2,NFE2L2,NQO1	3	Activated	biased	2.000	5.91E-03	2.06E-02	3-hydroxybutyric acid,fumaric acid,phosphorylethanolamine,sphingosine-1-phosphate	4 (6)	3	2 | 2	IU(2)	2 | 1	IU(1)	lipopolysaccharide	
TRIM39	transcription regulator	ERBB2,MYC,TP53,TRIM28	3	Activated		2.000	6.20E-03	2.32E-02	3-hydroxybutyric acid,fumaric acid,phosphorylethanolamine,sphingosine-1-phosphate	4 (4)	3	3 | 18	DU(4),IU(14)	3 | 2	IU(2)		
SOX4	chemical drug	AR,ERBB2,nandrolone decanoate,NQO1,Sod,TP53	3	Activated		2.000	6.20E-03	1.84E-02	3-hydroxybutyric acid,fumaric acid,phosphorylethanolamine,sphingosine-1-phosphate	4 (6)	3						
F11	other	CDKN1A,ERBB2,MYC,TP53,TRIM39	3	Activated		2.000	7.12E-03	2.27E-02	3-hydroxybutyric acid,fumaric acid,phosphorylethanolamine,sphingosine-1-phosphate	4 (5)	3						
	transcription regulator	CTNNB1,ERBB2,MYC,SOX4,SRC (family),TP53	3	Activated	biased	2.000	7.12E-03	4.03E-02	3-hydroxybutyric acid,fumaric acid,phosphorylethanolamine,sphingosine-1-phosphate	4 (6)	3	3 | 40	DU(26),IU(14)	3 | 6	DU(3),IU(3)	ERBB2,TGFB1	
	peptidase	ERBB2,F11,FN1,HGF,PLG,TGFB1	3	Activated	biased	2.000	7.12E-03	3.33E-02	fumaric acid,L-lactic acid,phosphorylethanolamine,sphingosine-1-phosphate	4 (6)	3	3 | 3	DU(1),IU(2)			F2	

Table S4: Demographic information of healthy and RRMS patients used for qualitative polymerase chain reaction data for metabolic genes presented in figure 2D.

	Healthy (N=10)	**RRMS (N=13)**
Female, N (%)	60%	77%
Mean age, years	43	44.9
Mean disease duration, years	--	4.5
DMTs	NA	None

DMTs, Disease modifying treatments; NA, not applicable; RRMS, Relapsing-remitting MS.

Table S5 Expression of glycolytic and TCA pathways.

Gene	GSE21942_ logFC	GSE21942_ AvgExpr	GSE21942_ Qvalue	GSE26484_ logFC	GSE26484_ AvgExpr	GSE26484_ Qvalue	GSE43591_ logFC	GSE43591_ AvgExpr	GSE43591_ Qvalue
CYB5D1	0.1287	5.9342	0.3118	-0.1821	6.4800	0.4786	0.0171	6.1754	0.9715
LDHA	-0.2243	11.2197	0.0028	-0.2239	11.8842	0.3717	0.1504	10.9657	0.4022
LDHB	0.1770	11.9221	0.1848	-0.5430	12.7474	0.1904	0.2044	12.2186	0.6115
SDHA	0.1009	9.5232	0.1228	-0.1829	10.1952	0.3164	-0.0697	9.4656	0.7440
SDHB	-0.0908	6.8039	0.4327	-0.1823	6.5173	0.4706	0.0234	6.7244	0.7664
SDHC	-0.0333	6.8356	0.3964	-0.1477	6.5249	0.6292	-0.0566	6.3450	0.7589
SDHD	0.1338	7.6226	0.3704	0.0840	8.5492	0.3411	0.0082	6.3840	0.7806
BDH1	0.0933	5.4385	0.5021	-0.0723	5.5455	0.3093	-0.0321	5.8018	0.8171
BDH2	0.0766	5.7171	0.5809	-0.2550	5.7514	0.4140	0.1352	5.5083	0.6956
MDH1	0.0712	9.8286	0.4118	-0.4106	10.7235	0.1695	0.1930	10.1793	0.4996
MDH2	-0.0854	8.5870	0.2267	-0.2279	8.9446	0.3660	-0.2095	8.2045	0.4655
ME1	0.0261	3.9952	0.8307	-0.0679	4.3624	0.6986	0.1270	3.5434	0.5635
ME2	-0.1859	8.7873	0.4000	-0.2928	9.0185	0.4980	-0.0391	8.1776	0.8730
ME3	0.0340	4.8949	0.6025	-0.0545	4.4121	0.7521	0.0616	5.1616	0.7351
ADSL	0.1284	9.4334	0.2071	-0.1267	10.0444	0.6812	0.1021	9.5433	0.8034
ASL	-0.2529	7.3667	0.0128	0.1420	7.5074	0.7265	-0.0517	6.2638	0.9272
FAH	-0.2045	4.8803	0.4180	0.0638	5.0523	0.8346	-0.0575	5.0459	0.6740
FH	-0.2252	7.1124	0.3832	-0.3020	6.3911	0.4514	0.0596	6.3813	0.8660
LDHAL6A	-0.0882	3.9150	0.2246	0.3616	4.7898	0.1607	0.0382	4.5353	0.8929
LDHAL6B	0.0367	2.8984	0.7242	0.0431	3.7392	0.8489	0.0613	2.9996	0.8016

We used 3 datasets from the National Center for Biotechnology Information (NCBI) Gene Expression Omnibus (GEO) database, including GSE21942, GSE26484, and GSE43591, and the raw data of each dataset was preprocessed with the Robust Multiarray Average (RMA) algorithm. Using Limma (or geo2R) differential expression analysis was performed on each dataset. Genes with an adjusted P-value lower than 0.05 considered as significant.

Animals

Female B6, SJL (10-12 weeks old) and 2D2 TCR (MOG_{35-55} specific TCR transgenic mice (Stock 006912) were purchased from the Jackson Laboratory (Bar Harbor, ME). Animals were housed in the pathogen-free animal facility of Henry Ford Hospital, Detroit, MI, according to the animal protocols approved by the Animal Care and Use Committee of Henry Ford Hospital.

EAE induction and recall response

B6, 2D2 and SJL mice (10-12 weeks old) were immunized on day 0 by subcutaneous injections in the flank region with a total 200 µl of emulsion containing antigen MOG_{35-55} or $PLP_{139-151}$ peptide (100 µg/mouse), along with killed Mycobacterium tuberculosis H37Ra (400 µg) in CFA as described previously (1-3). Pertussis toxin at the dose of 300 ng/mouse in PBS was given to B6 or 2D2 immunized mice on day 0 and 2 post-immunization in the volume of 200 µl. Pertussis toxin was not injected in SJL mice. One set of mice were injected with CFA/pertussis toxin without antigen/peptide named as control. Clinical disease was monitored daily in a blinded fashion by measuring paralysis according to the conventional grading system as described previously (1-3). Furthermore, cells (4×10^6/ml) isolated from spleens were cultured in the presence or absence of antigen (20 µg/ml). Cell proliferation and the production of various cytokines (IFNγ, GM-CSF, and IL17) were examined as described before (1-3).

Histopathology and Luxol fast blue staining

Hematoxylin and eosin and Luxol fast blue staining methods and histopathological analyses protocols were adopted from our reports (2, 4, 5). Mice were anesthetized with isoflurane and transcardially perfused with 0.9% chilled 1X PBS followed by 4% paraformaldehyde. Mouse spinal cord tissues were harvested and fixed in 4% paraformaldehyde for 24 hours at 4°C and later embedded in paraffin. Briefly, 5-µm spinal cord sections were obtained and stained with hematoxylin and eosin to check the infiltration of immune cells and the analysis of lesion size. Loss in white matter content and subsequent demyelination was visualized with Luxol fast blue staining. Brightfield images were captured using a light microscope, the demyelinated area was selected, measured and expressed as percentage of total area ([demyelinated area/total spinal cord area] × 100). Immunohistochemistry was performed on paraffin embedded spinal cord sections. Briefly, sections were deparaffinized, blocked and incubated with specific primary antibody (to CD4 and F4/80) overnight at 4°C. Sections were then washed 3 times with 0.1% PBST followed by incubation with an appropriate secondary antibody for 2 hours at room temperature. Thereafter, sections were rinsed, incubated with ABC reagent for 2 hours and visualized with 3,3′-diaminobenzidine. Images were acquired using a bright field microscope, converted into 8-bit images, threshold filtered and quantified using ImageJ software (National Institutes of Health, Bethesda, MD).

Flow cytometry

Surface markers of CNS-infiltrating or spleen cells were stained by incubating the cells with fluorochrome-labeled antibodies against Ly6C, F4/80, CD38 and EGR2 for 30 minutes at 4°C. MOG_{35-55}-specific activation of Th1 and Th17 from CNS-infiltrating lymphocytes were analyzed by stimulating the cells with the MOG_{35-55} peptide (20 ug/ml) for 18 hours followed by treatment with GolgiPlug at 37°C. After 5-hours of incubation, cells were processed for cell surface markers staining (CD3, CD4 and CD45) followed by intracellular markers staining by incubation with monoclonal antibodies against IFNγ and IL17 and GM-CSF as described before (2, 3).

Metabolomic analysis of RRMS and HS serum - Metabolomic profiling analysis was performed by Metabolon Inc. (Durham, NC).

Sample accessioning*:* Each sample received was accessioned into the Metabolon LIMS system and was assigned by the LIMS, a unique identifier that was associated with the original source identifier only. This identifier was used to track all sample handling, tasks, and results. The samples (and all derived aliquots) were tracked by the LIMS system. All portions of any sample were automatically assigned their own unique identifiers by the LIMS when a new task was created; these samples' relationship was also tracked. All samples were maintained at -80°C until processed.

***Sample preparation**:* Samples were prepared using the automated MicroLab STAR system from Hamilton Company. A recovery standard was added prior to the first step in the extraction process for QC purposes. To remove protein, dissociate small molecules bound to protein or trapped in the precipitated protein matrix, and to recover chemically diverse metabolites, proteins were precipitated with methanol under vigorous shaking for 2 minutes (Glen Mills GenoGrinder 2000) followed by centrifugation. The resulting extract was divided into 5 fractions: one for analysis by ultra-performance liquid chromatography-mass spectroscopy (UPLC-MS/MS) with positive ion mode electrospray ionization, one for analysis by UPLC-MS/MS with negative ion mode electrospray ionization, one for analysis by UPLC-MS/MS polar platform (negative ionization), one for analysis by gas chromatography-mass spectroscopy (GC-MS), and one sample was reserved for backup. Samples were placed briefly on a TurboVap (Zymark) to remove the organic solvent. For LC, the samples were stored overnight under nitrogen before preparation for analysis. For GC, each sample was dried under vacuum overnight before preparation for analysis.

Ultrahigh performance liquid chromatography-tandem mass spectroscopy (UPLC-MS/MS): The LC/MS portion of the platform was based on a Waters ACQUITY UPLC, and a Thermo Scientific Q-Exactive high resolution/accurate mass spectrometer interfaced with a heated electrospray ionization (HESI-II) source and Orbitrap mass analyzer operated at 35,000 mass resolution. The sample extract was dried then reconstituted in acidic or basic LC-compatible solvents, each of which contained 8 or more injection standards at fixed concentrations to ensure injection and chromatographic consistency. One aliquot was analyzed using acidic positive ion optimized conditions and the other using basic negative ion optimized conditions in 2 independent injections using separate dedicated columns (Waters UPLC BEH C18-2.1x100 mm, 1.7 µm). Extracts reconstituted in acidic conditions were gradient eluted from a C18 column using water and methanol containing 0.1% formic acid. The basic extracts were similarly eluted from C18 using methanol and water, however, with 6.5mM Ammonium Bicarbonate. The third aliquot was analyzed via negative ionization following elution from a HILIC column (Waters UPLC BEH Amide 2.1x150 mm, 1.7 µm) using a gradient consisting of water and acetonitrile with 10mM Ammonium Formate. The MS analysis alternated between MS and data-dependent MS^2 scans using dynamic exclusion, and the scan range was from 80-1000 *m/z*. Raw data files are archived and extracted as described below.

Gas chromatography-mass spectroscopy (GC-MS): The samples destined for analysis by GC-MS were dried under vacuum for a minimum of 18 h prior to being derivatized under dried nitrogen using bistrimethyl-silyltrifluoroacetamide. Derivatized samples were separated on a 5% diphenyl/95% dimethyl polysiloxane fused silica column (20 m x 0.18 mm ID; 0.18 um film thickness) with helium as a carrier gas and a temperature ramp from 60° to 340°C in a 17.5 min period. Samples were analyzed on a Thermo-Finnigan Trace DSQ fast-scanning single-quadrupole mass spectrometer using electron impact ionization (EI) and operated at unit mass resolving power. The scan range was from 50–750 m/z. Raw data files are archived and extracted as described below.

Quality assurance/quality control: Several types of controls were analyzed in concert with the experimental samples: a pooled matrix sample generated by taking a small volume of each experimental sample (or alternatively, use of a pool of well-characterized human plasma) served as a technical replicate throughout the data set; extracted water samples served as process blanks; and a cocktail of QC standards that were carefully chosen not to interfere with the measurement of endogenous compounds were spiked into every analyzed sample, allowed instrument performance monitoring and aided chromatographic alignment. Instrument variability was determined by calculating the median relative standard deviation (RSD) for the standards that were added to each sample prior to injection into the mass spectrometers. Overall process variability was determined by calculating the median RSD for all endogenous metabolites (i.e., non-instrument standards) present in 100% of the pooled matrix samples. Experimental samples were randomized across the platform run with QC samples spaced evenly among the injections.

Data extraction and compound identification: Raw data was extracted, peak-identified, and QC processed using Metabolon's hardware and software. These systems are built on a web-service platform utilizing Microsoft's.NET technologies, which run on high-performance application servers and fiber-channel storage arrays in clusters to provide active failover and load-balancing. Compounds were identified by comparison to library entries

of purified standards or recurrent unknown entities. Metabolon maintains a library based on authenticated standards that contain the retention time/index (RI), mass to charge ratio (*m/z)*, and chromatographic data (including MS/MS spectral data) on all molecules present in the library. Furthermore, biochemical identifications are based on 3 criteria: retention index within a narrow RI window of the proposed identification, accurate mass match to the library +/- 0.005 amu, and the MS/MS forward and reverse scores between the experimental data and authentic standards. The MS/MS scores are based on a comparison of the ions present in the experimental spectrum to the ions present in the library spectrum. While there may be similarities between these molecules based on one of these factors, the use of all 3 data points can be utilized to distinguish and differentiate biochemicals. More than 3300 commercially available purified standard compounds have been acquired and registered into LIMS for distribution to both the LC-MS and GC-MS platforms for the determination of their analytical characteristics. Additional mass spectral entries have been created for structurally unnamed biochemicals, which have been identified by virtue of their recurrent nature (both chromatographic and mass spectral). These compounds have the potential to be identified by the future acquisition of a matching purified standard or by classical structural analysis.

Curation: A variety of curation procedures were carried out to ensure that a high-quality data set was made available for statistical analysis and data interpretation. The QC and curation processes were designed to ensure accurate and consistent identification of true chemical entities and to remove those representing system artifacts, misassignments, and background noise. Metabolon data analysts use proprietary visualization and interpretation software to confirm the consistency of peak identification among the various samples. Library matches for each compound were checked for each sample and corrected if necessary.

Metabolite quantification and data normalization: Peaks were quantified using area-under-the-curve. For studies spanning multiple days, a data normalization step was performed to correct variation resulting from instrument inter-day tuning differences. Essentially, each compound was corrected in run-day blocks by registering the medians to equal one (1.00) and normalizing each data point proportionately (termed the "block correction"). For studies that did not require more than one day of analysis, no normalization is necessary, other than for purposes of data visualization. In certain instances, biochemical data may have been normalized to an additional factor (e.g., cell counts, total protein as determined by Bradford assay, osmolality, etc.) to account for differences in metabolite levels due to differences in the amount of material present in each sample.

Methodology for the quantitation of 2-DG-6P using LC-MS/MS

Chemicals and reagents: 2-deoxy-D-Glucose-6-phosphate (sodium salt)standard was obtained from Cayman (Ann Arbor, MI) and isotopically labeled 2-deoxy-D-[UL-13C6]glucose-6-phosphate, used as an internal standard (ISTD), were purchased from Omicron Biochemicals Inc (South Bend, IN). Acetonitrile (HPLC-grade), Formic acid, Hexane, MS grade water and Methanol were purchased from Sigma Aldrich (St Louis, MO).

Experiments: Concentrated stock solutions of 2-deoxy-D-Glucose-6-phosphate (2DG-6P)(10 µg/mL) and the ISTD (250 µg/mL) were prepared in a 1:1 water:acetonitrile solution. Working solutions were prepared in matrix ranged from 4–1000 ng/mL for 2 DG-6P. An ISTD working solution (0.625 ng/mL) was prepared in the extraction solvent 1:1 Water: acetonitrile containing 1% formic acid. Calibration curve standards were prepared in duplicate for absolute concentration, while QC and blank (non-spiked) samples were prepared in Triplicates.

Sample Preparation and extraction: Sample preparation for Quantitation of 2-DG-6P from Spinal cord sample [25mg each] for performed using the following in-house method for extraction. Liquid nitrogen frozen samples were crushed with Mini Mortar and Pestle to a fine powder, followed by addition 300 ul of 1:1 Water: Acetonitrile solution and vigorous vertexing for 60 seconds twice. 10 ul of ISTD (^{13}C-2DG-6P) stock (1ug/mL) was added in the above mixture for recovery and matrix effect. Samples were further sonicated in water bath for 30 seconds followed by centrifugation for 15 minutes at 15,000g at 4°C. The upper phase (~250 µl) containing the extracted matrix was transferred into fresh tubes, followed by addition of an equal amount of LCMS grade Hexane, followed by collection of aqueous layer (~200 µl) into fresh tubes. Collected liquid were dried completely by

nitrogen gas at 37°C. The dried residue was resuspended in 100 µl diluent (Waters: Acetonitrile), vortexed and centrifuge (15 minutes at 15,000g at 4°C), and placed in an autosampler vial for LC-MS analysis.

LC-MS/MS instrumentation and conditions: Waters UPLC connected to Acquity TQD mass spectrometry was employed for method development including the LC method optimization, ionization, and fragmentation tests. UPLC was configured with a binary pump, a thermostatted column compartment, and a temperature controlled autosampler. The binary pump was used to transport mobile phase A (Water 5mM ammonium acetate + 0.1% liquid ammonia) and B (Methanol +0.1% liquid ammonia) at a flow rate of 0.3 ml/min in gradient mode. Best separation of 2-DG-6P was achieved using UPLC with auto sampler with reversed-phase waters XBridge BEH Amide Column, 130Å, 3.5 µm, 4.6 mm X 150 mm with in-line filter and guard kept at 50 ^{0}C. Mobile phase linear gradient A and B was programed and described in Table 2 for 2DG-6P separation. The flowrate was set to 500 ul/min with an overall runtime of 6 minutes. The autosampler was maintained at 4°C, and the injection volume was 5 µl with total running time of 7 minutes.

TQD mass spectrometry was operated at Electrospray Ionization mode. The column effluent was monitored by negative ion electrospray (ESI-) using multiple reaction monitoring (MRM). The primary and confirmatory MRM transitions used for 2DG-6P and its ISTD, with their respective optimized settings, are listed in Table 1. The parameters for TQD mass spectrometry equipped with a ESI probe: Capillary: voltage, 3.5 kV for negative mode: Source temp : 120 °C :Desolvation temp: 450 °C; Cone gas flow: 150 L/Hr : Desolvation gas flow:1000 L/Hr Collision gas flow: 0.25 mL/min and Nebulizer gas flow: 7 Bar. For 2DG-6P quantification, peak area ratios (PARs) of the analyte peak area to the ISTD peak were calculated. The calibration curve, prepared in control matrix, was constructed using PARs of the calibration samples by applying a one/concentration weighting (1/x) linear regression model. All QC sample concentrations were then calculated from their PARs against the calibration curve.

Method validation: Limit of detection (LOD) and Lower Limit of Quantification (LLOQ): Nine calibration standards ranging from 4-1000ng/ml was subjected to the full extraction procedure three times before analysis. The limit of detection (LOD) was defined as the 2DG6P concentration corresponding to the lowest calibration point, where signal to noise ratio (s/n) was three times greater than from the blank signal and lower limit of quantification was signal 10 times more compared to s/n with blank.

Precursor	Selected MRM Precursor >Fragment	Collision energy	Cove voltage	
243.1	243.1>97	15	35	Primary
243.1	243.1>79	15	32	Confirmatory
249.1	249.1>103	13	35	Primary
249.1	249.1>85	23	35	Confirmatory

Selected 2DG6P MRM transitions with parameters and chromatographic retention.

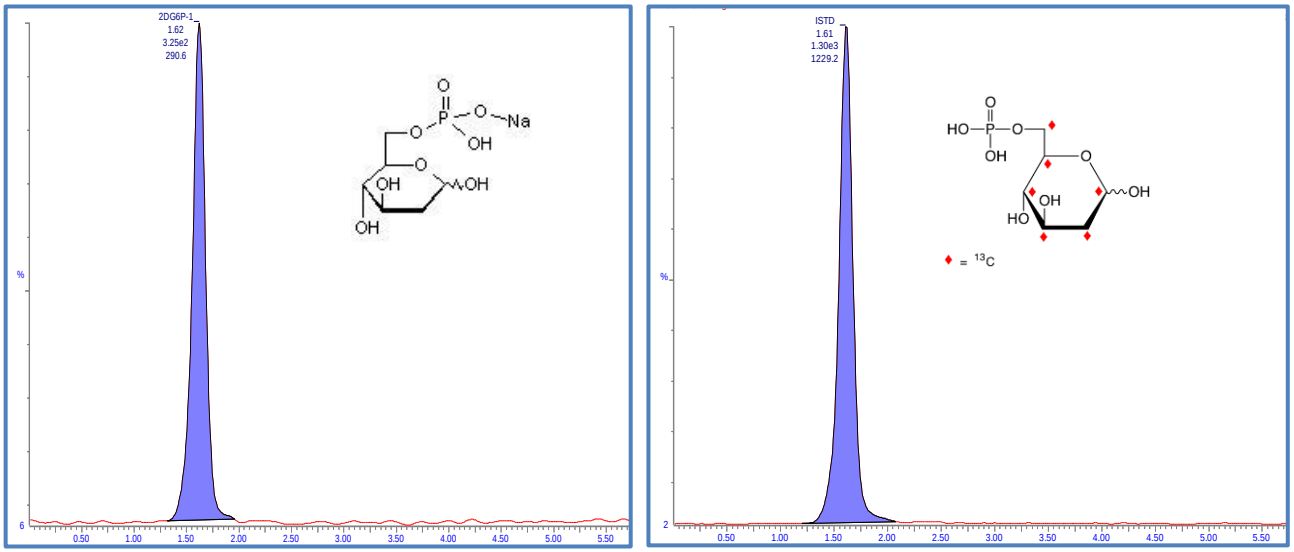

UPLC separation of DG6Pand its isotopically labeled internal standard (ISTD), using aXBridge BEH Amide Column, 130Å, 3.5 µm, 4.6 mm X 150 mm

Time(min)	Flow Rate (mL/Min)	%A	%B	Curve
0.0	0.6	60	40	6
1.0	0.6	60	40	6
2.0	0.6	80	20	6
4.0	0.6	80	20	6
4.1	0.6	60	40	6
6.0	0.6	60	40	6

Optimized gradient run for separation and quantitation of 2-DG-6P in MRM mode

Data analysis: Mass spectrometric data was acquired by MassLynx v4.2software. Quantification software: TargetLynxsoftware was used for preparing the calibration curve and absolute quantitation of 2DG6P in the samples. Analyte concentrations were calculated using a 1/x weighted linear regression analysis of the standard curve.

Quantitative Performance: The quantitative performance using this sample preparation and LC-MS method was excellent, achieving a LLOQ of 4 ng/mL for 2DG6P. Calibration curves were linear (r2 > 0.996) from 4.–1000 ng/mL with accuracies between 85–115% with CVs.

Mouse and human primers sequences for qPCR:

mGlut1-F CAGTTCGGCTATAACACTGGTG
mGlut1-R GCCCCCGACAGAGAAGATG
mHK2-F CTTACCGTCTGGCTGACCAACAC
mHK2-R CTCCATTTCCACCTTCATCCTTCT
mTPI-F CCAGGAAGTTCTTCGTTGGGG
mTPI-R CAAAGTCGATGTAAGCGGTGG
mPKM-F GCCGCCTGGACATTGACTC
mPKM-R CCATGAGAGAAATTCAGCCGA
mLDHA-F CATTGTCAAGTACAGTCCACACT
mLDHA-R TTCCAATTACTCGGTTTTTGGGA
mMCT1-F GACCATTGTGGAATGCTGCCCT
mMCT1-R CGATGATGAGGATCACGCCACA

hSDHA-F GAGATGTGGTGTCTCGGTCCAT
hSDHA-R GCTGTCTCTGAAATGCCAGGCA
hSDHB-F GCAGTCCATAGAAGAGCGTGAG
hSDHB-R TGTCTCCGTTCCACCAGTAGCT
hSDHC-F GGTTCAAACCGTCCTCTGTCTC
hSDHC-R CGACATGCCAAAAAGAGAGACCC
hSDHD-F GCAGCACATACACTTGTCACCG
hSDHD-R GGGAATAGTCCATCGCAGAGCA
hLDHA-F GGATCTCCAACATGGCAGCCTT
hLDHA-R AGACGGCTTTCTCCCTCTTGCT
hLDHB-F GGACAAGTTGGTATGGCGTGTG
hLDHB-R AAGCTCCCATGCTGCAGATCCA
hME1-F GGAGTTGCTCTTGGTGTTGTGG
hME1-R GGATAAAGCCGACCCTCTTCCA
hME2-F ATCCTACAGCACAGGCAGAGTG
hME2-R TGACCTGGTGTAAAGACTCGCC
hME3-F AATGCCTTCCGCCTGCTCAACA
hME3-R TGGTGATTCGCAGAGCAGCCAA
hMDH1-F CGGTGTCCTAATGGAACTGCAAG
hMDH1-R CATCCAGGTCTTTGAAGGCAACG
hMDH2-F CTGGACATCGTCAGAGCCAACA
hMDH2-R GGATGATGGTCTTCCCAGCATG

References:

1. Mangalam A, *et al.* (2013) Profile of circulatory metabolites in a relapsing-remitting animal model of multiple sclerosis using global metabolomics. *J. Clin. Cell. Immunol.* 4: 1000150.
2. Mangalam AK, *et al.* (2016) AMP-Activated Protein Kinase Suppresses Autoimmune Central Nervous System Disease by Regulating M1-Type Macrophage-Th17 Axis. *J Immunol* 197(3):747-760.
3. Poisson LM, *et al.* (2015) Untargeted Plasma Metabolomics Identifies Endogenous Metabolite with Drug-like Properties in Chronic Animal Model of Multiple Sclerosis. *The Journal of biological chemistry* 290(52):30697-30712.
4. Khan MB, *et al.* (2015) Remote ischemic postconditioning: harnessing endogenous protection in a murine model of vascular cognitive impairment. *Transl Stroke Res* 6(1):69-77.
5. Vaibhav K, *et al.* (2018) Remote ischemic post-conditioning promotes hematoma resolution via AMPK-dependent immune regulation. *J Exp Med* 215(10):2636-2654.